Energy & Environmental Science

Accepted Manuscript

ROYAL SOCIETY OF CHEMISTRY

www.rsc.org/ees

Operando electrochemical NMR microscopy of polymer fuel cells

A.S. Cattaneo[1], D.C. Villa[1], S. Angioni[1], C. Ferrara[1], R. Melzi[2], E. Quartarone[1] and P. Mustarelli[1,*]

[1]Dept. of Chemistry and INSTM, University of Pavia, Via Taramelli 16, 27100 Pavia, Italy

[2] Bruker Biospin Italia, Viale Lancetti 43, 20158 Milano, Italy.

*Correspondence to: piercarlo.mustarelli@unipv.it

Abstract

The design of high-temperature polymer fuel cells (PEMFCs), e.g. those expected for automotive applications, requires a deep understanding of the electrochemical reactions occurring in the device during operation. *Operando* Electrochemical Nuclear Magnetic Resonance Microscopy can constitute a powerful investigation tool to this aim. At present, however, some strong technical limitations, like low sensitivity to less mobile protons, and limited temperature range of analysis, have bound its use to case models based on perfluorinated membranes operating at high relative humidity and low temperature. By means of a suitable design of the experimental set-up and the use of a new 3D acquisition protocol, we proved the feasibility of electrochemical NMR microscopy on low-water containing polybenzimidazole-based devices, so allowing full *operando* characterization of high-temperature PEMFCs, and also paving the way to applications to other electrochemical devices, such as batteries, sensors, supercapacitors, etc.

The implementation of *operando* measurements based on spectroscopic, microscopic and diffraction methods is emerging as a mandatory approach for full exploitation of the potential of functional materials and related electrochemical devices. During the last years, this approach was first applied to the investigation of materials for heterogeneous catalysis,[1-3] and then to the investigation of lithium batteries.[4-9] Electrochemical reactions at solid-gas interfaces, which are of great interest for metal-air batteries, water splitting devices and fuel cells, were also the object of careful studies.[5,9-11]

Nuclear Magnetic Resonance Imaging (MRI) at the microscopic level underwent fast development during ’90s and was rapidly recognized as a powerful tool for materials investigations.[12] More recently, it was applied to the characterization of interfaces and full devices, even under *operando* conditions. Grey’s and Jerschow’s groups applied this approach to address the microstructure in Li-

ion batteries and in capacitors under operation.[13-14] The application on Li/Na batteries, however, is made difficult by the paramagnetic and conducting nature of some cell components, e.g. graphite anode and transition metal cathode, as well as by the presence of the current collectors.

In the recent past, a great deal of attention was devoted to the investigation (by means of both MRI and other *operando* techniques) of proton exchange membrane fuel cells (PEMFCs),[15] which are of interest chiefly for automotive applications.[16] Since a correct water management is mandatory to achieve high power density, long-term operation and good robustness, investigation of water content and distribution plays a crucial role in the engineering process of these devices. A seminal work on this topic dating back to 1995 is due to Watanabe's group.[17] To investigate these fundamental aspects, several magnetic resonance techniques were employed, e.g. Electron Paramagnetic Resonance (EPR),[18] and electrophoretic NMR.[19] Also Pulse Field Gradient (PFG)-NMR was used for studying proton mobility in systems of interest for fuel cells.[20] However, with a few exceptions, these works dealt with PEMCFs based on Nafion® or other sulphonated polymers, whose working temperature is around 80°C and where a consistent amount of water is required for proper operation. Whereas "high-temperature PEMFCs" mainly based on other polymers, such as polybenzimidazole, work in the range 120-200°C and are characterized by a significantly lower amount of water, whose distribution can be then difficult to investigate.

Coming back to MRI, careful studies on this topic were performed by Hirai in Japan[21-26] and Wasylishen in Canada.[27-31] A good review of the state-of-the-art was recently reported by Han.[32] The main problems of MRI application to PEMFCs are related to the presence of metallic (bipolar plates) and semiconducting (carbon-based gas diffusion layers, GDL) materials, which can lead to artifacts and/or signal degradation due to parasitic currents and bulk susceptivity. Other relevant problems are caused by the intrinsic low sensitivity of the technique regarding bonded or less mobile protons, which possess short spin-spin relaxation time (T_2). This limitation affects the minimum amount of proton density really detectable during the measurement and, indirectly, the spatial resolution. As a matter of fact, nearly all the studies published up to now were performed by using 2D spin-echo (SE) sequences. Within this approach, at a given field of view (FOV), any attempt to increase the spatial resolution, through reduction of the FOV or increase of the voxel matrix dimension, would lead, due to hardware limitations, to a direct increase of the minimum accessible time of echo (TE). Such a technical disadvantage generates an obvious conflict when observing strongly interacting systems, which are typically characterized by short T_2. This actually limited MRI investigations to fuel cells based on perfluorinated membranes (e.g. Nafion®) operating near room temperature and at high relative humidity (about 100%). However, due to the

great interest grown on high-temperature PEMFCs such as those based on polybenzimidazole (PBI) membranes,[33-34] it is mandatory to overcome these limitations and to widen the *operando* MRI investigations also to materials requiring much less water for their working. PBIs constitute a class of thermoplastic polymers, having high thermal and mechanical stability, where proton conductivity can be obtained through a doping with phosphoric acid. Their use in fuel cells was pioneered by Wainright et al.,[35] and Li et al..[36] Significant developments were also due to the group of Benicewicz.[37-38]

Our main goal, here, was to give a feasibility proof of *operando* ^{1}H electrochemical NMR microscopy (ELectrochemical MIcroscope NMR, ELMINMR in the following), which is independent on the nucleus relaxation rates, without any relevant limitation on the operating temperature and actual humidity of the investigated device. This was obtained thanks to a careful design of the experimental set-up–and to the use of a new zero-time echo (ZTE) 3D acquisition sequence, recently developed by Weiger et al.[39-41]

In this frame, we chose to investigate PBI-based PEMFCs since our main goal here is to demonstrate that ELMINMR can be successfully used for studies in low-humidity environments. The choice to work below 100°C was mainly dictated by practical reasons, however it does not impact on our main goal, but only on the proton mobility of the proton species present in our system. We also stress that, at present, we do not distinguish among different proton populations, chiefly water and phosphoric acid. This will require the use of a chemical shift imaging (CSI) protocol, where a ^{1}H NMR spectrum is acquired for selected voxels, in order to build a chemical mapping of the single proton species. The implementation of this method on PEMFCs will be addressed in future works.

Figure 1 reports a scheme of the ELMINMR apparatus, which is mainly based on the integration of two subsystems: a commercial NMR spectrometer equipped with microimaging accessory, and a potentiostat/galvanostat with a current booster to allow high density power in the electrochemical device under study, in our case a membrane-electrode-assembly (MEA) for a PEMFC. Here, the heart of the apparatus is a customized probe (ELMI) combining: i) a commercial birdcage resonator, ii) an electrical circuit for MEA polarization, and iii) the inlet/outlet circuitry of hydrogen and oxygen (air) (see ESI and Fig. S1). The main problems to solve were the heating of the cell, and the management of the metallic/semiconducting parts inside the probe (carbon cloths, gas diffusion layers, etc.). The first problem was solved by heating the gases outside the NMR magnet: a small plastic pipeline for each gas was built from gas source to PEMFC located inside the magnet and was immerged in a heating bath. This allowed us to avoid direct Joule heating of gases into the ELMI probe, which can be also hazardous because of hydrogen. Concerning the second point, we

initially developed an inductively-coupled NMR surface coil directly facing the MEA (Figs. S6-S7), in order to maximize the signal-to-noise ratio. However, this solution originated strong artifacts (Fig. S8) and was discarded. Therefore, as the NMR coil we decided to use a standard birdcage resonator and developed a Teflon® cell for MEA housing (Figs. S2-S3), which can fit inside it. The membrane used for MEA assembly was obtained with a spray method from a pyridine-based polybenzimidazole (PBI_5N) solution.[42-43] The cell active area was about 2 cm^2 (see ESI). The cell electrodes were connected to current collectors just outside the housing, so avoiding their presence in the FOV of ZTE images. As a result, a good S/N ratio was achieved.

Due to the presence of spin populations with short spin-spin relaxation time T_2 (e.g. proton of polymer backbone and of weakly-bonded phosphoric acid), the usual multi-slice multi-echo (MSME) MRI acquisition sequence, as already stated, is not well suited. Therefore, we exploited a relatively new 3D imaging sequence called ZTE, able to target also short-T_2 samples, which was developed to study hard tissues like teeth and bones.[40-41] ZTE is achieved by 3D radial centre-out encoding and hard-pulse radiofrequency (RF) excitation while the projection gradient is already on.[31] More technical details, as well as a comparison between a spin echo and a ZTE image recorded for the same sample are given in ESI.

Figure 2 shows the *operando* ^{1}H microimaging study of a PBI_5N fuel cell operated for seven hours at 80°C @ 30 mA. The a) image was taken before starting the cell operation, in order to observe eventual abnormalities in the adsorbed water distribution. Water is both on the active part of the cell and on the electrodes (see axial slices), where it particularly resides on the borders. The intense rectangular shape is due to the o-rings protons. The presence of water before operation is not surprising. In fact, even if MEA was previously dried at 120°C for 2h in order to remove all water coming from the doping procedure, the entire MEA is highly hygroscopic and during the cell assembly has time enough to collect some water from air. After reaching 80°C, we started to operate the cell at constant current (30 mA). The b) image was recorded in 17 minutes just after the start. At this temperature the gas flows removed nearly all adsorbed water. The cell was able to work for 7 hours showing a voltage oscillating around 0.44V, without any failure. We can observe that after 420 minutes (image c) a very small amount of water is present. By exploiting axial slices, obtained from the 3D dataset using the Jive package included in Bruker software, we can focus our attention mainly on the squared small active part of the cell. In this region we see no water at t=0, but a small amount of water after seven working hours (images b and c, respectively). This water seems to be located mainly on the anode side, which can be due to humidity from gas inlets or to cathode back-diffusion as already reported.[44] We stopped the cell after this step and let the system to freely cool down, without removing it from the magnet. The next day we measured the fuel cell

again (Fig. 2.d), observing that the moisture coming from the gases circuit has condensed on the MEA. Anyway, it seems that this adsorbed water is not detrimental for cell performances, because the cell was still able to operate for hours at 80°C at 30 mA with a voltage ~0.44V.

In order to fully explore the potential of the ZTE protocol, we also performed a study under low air flow (2L/min instead of 5L/m), low temperature (35°C) and low polarization current (5mA). Under these conditions the behavior of the PBI_5N MEA is indeed not optimal, and we observed a quick failure of cell performances in just four hours, with a voltage decrease from 0.44V to 0.31V under constant current. Figure 3 describes this study with three images, taken before the operation at 35°C (a), after one (b) and two hours of operation (c). The a) ZTE image suggests that 35°C are enough for removing the water adsorbed into the fuel cell during assembly, but the axial slices taken for the central part, where the active square is located, revealed that this part is still wet. After one hour the active part is free from water, but electrodes and gas grids start to accumulate water (b). After two hours, also some water is detectable in the central part of the cell (c).

The same cell was used for a final study at 47°C. The ^{1}H microimaging results are reported in Figure 4. The water stored on the electrodes increases after just 10 minutes of operation (image b) and it still present in the central active part after 75 minutes. The cell also showed a decrease in voltage, which dropped from 0.43V to 0.33V. After about four hours the cell stopped working properly, as evidenced by the low voltage and the absence of water formed.

We stress that our main aim here, was to give a proof-of-concept of the feasibility of the ELMINMR instrument, rather than reporting full scientific results and their thorough discussion. The application of this new apparatus to PBI-based MEAs for fuel cells was clearly demonstrated. For the first time, we were able to investigate the proton distribution in membranes at low humidity level, as those expected to be used in automotive, while previously analysis was limited to Nafion®-based membranes operating at 100% RH. As already stated, at this stage we did not distinguish between proton from water and from phosphoric acid, which is also present in the MEA. This did not allow a full understanding of water formation details, although, at least from a qualitative point of view, we are confident that the density maxima of Figs. 1-3 are due to water.

Our results pave the way to the development of a powerful diagnostic approach to investigate water production and its management in fuel cells operating at high temperature and low humidity conditions, such as the ones designed for automotive. A piece of fundamental knowledge may also be obtained through a total or selective isotopic enrichment of the samples with ^{2}H. This could provide a unique opportunity to investigate diffusion and exchange processes among polymer matrix, phosphoric acid and water. Finally, we can foresee the application of the electrochemical NMR microscopy to a wide range of electrochemical devices, including fuel cells, sensors,

batteries, supercapacitors, and photovoltaic modules, in case by exploiting other abundant spin-½ nuclei such as ^{19}F and ^{31}P.

References

1 A. Vimont, F. Thibault-Starzyk, and M. Daturi, *Chem. Soc. Rev.* 2010, **39**, 4928-4950.

2 I. E. Wachs and C. A. Roberts, *Chem. Soc. Rev.* 2010, **39**, 5002-5017.3

3 A. A. Lysova and I. V. Koptyug, *Chem. Soc. Rev.* 2010, **39**, 4585-4601.

4 X. Liu, D. Wang, G. Liu, V. Srinvasan, Z. Liu, Z. Hussain and W. Yang, *Nat. Commun*. 2013, **4**, 2568.

5 L. Li, Y.-C. K. Chen-Wiegart, J. Wang, P. Gao, Q. Ding, Y.-S. Yu, F. Wang, J. Cabana, J. Wang and S. Jin, *Nat. Commun.* 2015, **6**, 6883.

6 D. P. Finegan, M. Scheel, J. B. Robinson, B. Tjaden, I. Hunt, T. J. Mason, J. Millichamp, M. Di Michiel, G. J. Offer, G. Hinds, D. J. L. Brett and P. R. Shearing *Nat. Commun*. 2015, **6**, 6924.

7 F. Blanc, M. Leskes and C .P. Grey, *Acc. Chem. Res.* 2013 **46** (9), 1952-1963.

8 M. Klett, M. Giesecke, A. Nyman, F. Hallberg, R. Wreland Lindström, G. Lindbergh and I. Furó, *J. Am. Chem. Soc.* 2012, **134**, 14654-14657.

9 G. Gershinsky, E. Bar, L. Monconduit and D. Zitoun, *Energy Environ. Sci.* 2014, **7**, 2012-2016.

10 Z. A. Feng, F. El Gabaly, X. Ye, Z.-X. Shen and W. C. Chueh, *Nat. Commun.* 2014, **5**, 4374.

11 D. N. Mueller, M. L. MacHala, H. Bluhm and W. C. Chueh, *Nat. Commun.* 2015, **6**, 6097.

12 B. Blümich, NMR Imaging of Materials, Oxford University Press, New York, (2000).

13 S. Chandrashekar, N. M. Trease, C. P. Grey and A. Jerschow, *Nat. Mater.* 2012, **11**, 311-315.

14 A. J. Ilott, N. M. Trease, C. P. Grey and A. Jerschow, *Nat. Commun.* 2014, **5**, 4536.

15 S. Deabate, G. Gebel, P. Huguet, A. Morin and G. Pourcelly, *Energy Environ. Sci.* 2012, **5**, 8824-8847.

16 U. Eberle, B. Müller and R. von Helmolt, *Energy Environ. Sci.* 2012, **5**, 8780-8798.

17 M. Watanabe, H. Igarashi, H. Uchida and F. Hirasawa, *J. Electroanal. Chem.* 1995, **399**, 239-241.

18 B. Vogel, E. Aleksandrova, S. Mitov, M. Krafft, A. Dreizler, J. Kerres, M. Hein and E. Roduner, *J. Electrochem. Soc.* 2008, **155**, B570-B574.

19 M. Ise, K. D. Kreuer and J. Maier, *Solid State Ionics* 1999, **125**, 213-223.

20 M. Schuster, W. H. Meyer, G. Wegner, H. G. Herz, M. Ise, M. Schuster, K. D. Kreuer and J. Maier, *Solid State Ionics* 2001, **145**, 85-92.

21 S. Tsushima, K. Teranishi and S. Hirai, *Electrochem. Solid State Lett.* 2004, **7**, A269-A272.

22 K. Teranishi, S. Tsushima and S. Hirai, *Electrochem. Solid State Lett.* 2005, **8**, A281-A284.

23 K. Teranishi, S. Tsushima, K. Nishida and S. Hirai, *Magn. Reson. Imaging* 2005, **23**, 255-258.

24 S. Tsushima, S. Hirai, K. Kitamura, M. Yamashita and S. Takase, *Appl. Magn. Reson*. 2007, **32**, 233-241.

25 S. Tsushima and S. Hirai, *Fuel Cells* 2009, **5**, 506-517.

26 S. Tsushima and S. Hirai, *Progress in Energy and Combustion Science*, 2011, **37**, 204-220.

27 K. W. Feindel, L. P.-A. LaRocque, D. Starke, S. H. Bergens and R. E. Wasylishen, *J. Am. Chem. Soc.* 2004, **126**, 11436-11437.

28 K. W. Feindel, S. H. Bergens and R. E. Wasylishen, *J. Am. Chem. Soc.* 2006, **128**, 14192-14199.

29 K. W. Feindel, S. H. Bergens and R. E. Wasylishen, *ChemPhysChem.* 2006, **7**, 67-75.

30 K. W. Feindel, S. H. Bergens and R. E. Wasilishen, *Phys. Chem. Chem. Phys*. 2007, **9**, 1850-1857.

31 M. Wang, K. W. Feindel, S. H. Bergens and R. E. Wasylishen, *J. Power Source*s 2010, **195**, 7316-7322.

32 O.H. Han, *Prog. Nucl. Magn. Reson. Spectroscop.* 2013, **72**, 1-41.

33 J. A. Asensio, E. M. Sànchez and P. Gòmez-Romero, *Chem. Soc. Rev.* 2010, **39,** 3210-3239.

34 E. Quartarone and P. Mustarelli, *Energy Environ. Sci.* 2012, **5**, 6436-6444.

35 J. S. Wainright, J.-T. Wang, D. Weng, R. F. Savinell and M. Litt, *J. Electrochem. Soc.* 1995, **142**, L121-L123.

36 Q. Li, R. He, J. O. Jensen and N. J. Bjerrum, *Chem. Mater.* 2003, **15**, 4896-4915.

37 L. Xiao, H. Zhang, E. Scanlon, L. S. Ramanathan, E.-W. Choe, D. Rogers, T. Apple and B. C. Benicewicz, *Chem. Mater.* 2005, **17**, 5328-5333.

38 S. Yu, L. Xiao and B. C. Benicewicz, *Fuel Cells* 2008, **8**, 165-174.

39 M. Weiger, K. P. Preussmann and F. Hennel, *Magn. Reson. Med.* 2011, **66**, 379-389.

40 M. Weiger, K. P. Preussman, A.-K. Bracher, S. Kohler, V. Lehmann, U. Wolfram, F. Hennel, V. Rasche, *NMR Biomed*, 2012, **25**, 1144-1151.

41 M. Weiger, M. Stampanoni, K. P. Pruessmann, *Bone* 2013, **54**, 44-47.

42 A. Carollo, E. Quartarone, C. Tomasi, P. Mustarelli, F. Belotti, A. Magistris, F. Maestroni, M. Parachini, L. Garlaschelli and P. P. Righetti, *J. Power Sources* 2006, **160**, 175-180.

43 E. Quartarone, D. C. Villa, S. Angioni and P. Mustarelli, *Chem. Comm.* 2015, **51**, 1983-1986.

44 Z. Dunbar and R. I. Masel, *J. Power Sources* 2007, **171**, 678-687.

Acknowledgments

We gratefully acknowledge the financial help of Fondazione Cariplo (Milano, grant n.2011/1812). We also thank F. Moneta (Bruker Biospin) for technical support and useful discussions.

A.S.C. and C.F. performed MRI measurements, S.A. prepared MEAs, D.C.V. assembled the electrochemical apparatus, R. M. developed some parts of the ELMI probe, E. Q. and P. M. conceived the experiments, P.M. and A.S.C. wrote the paper, all the Authors contributed to the paper.

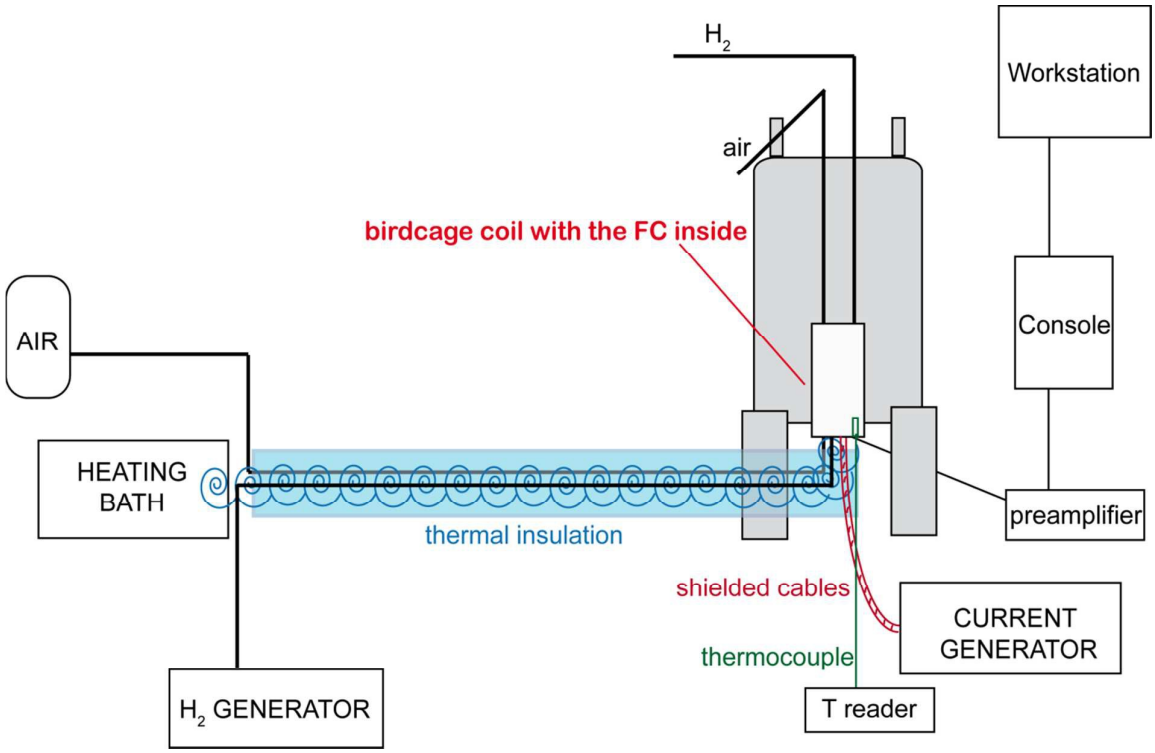

Fig. 1 Scheme of ELMINMR apparatus. ^{1}H MRI images were recorded using a 400 MHz spectrometer interfaced with an Avance III Bruker console, equipped with microimaging accessory and a 30 mm birdcage resonator. Inside the birdcage, a Teflon® cylinder hosted the fuel cell. The fuel H_2/air gases were heated through a heating bath in a pipeline and provided to the cell from the bottom of the magnet. The polarization current was provided through shielded cables. The internal FC temperature was monitored with a thermocouple near to the MEA.

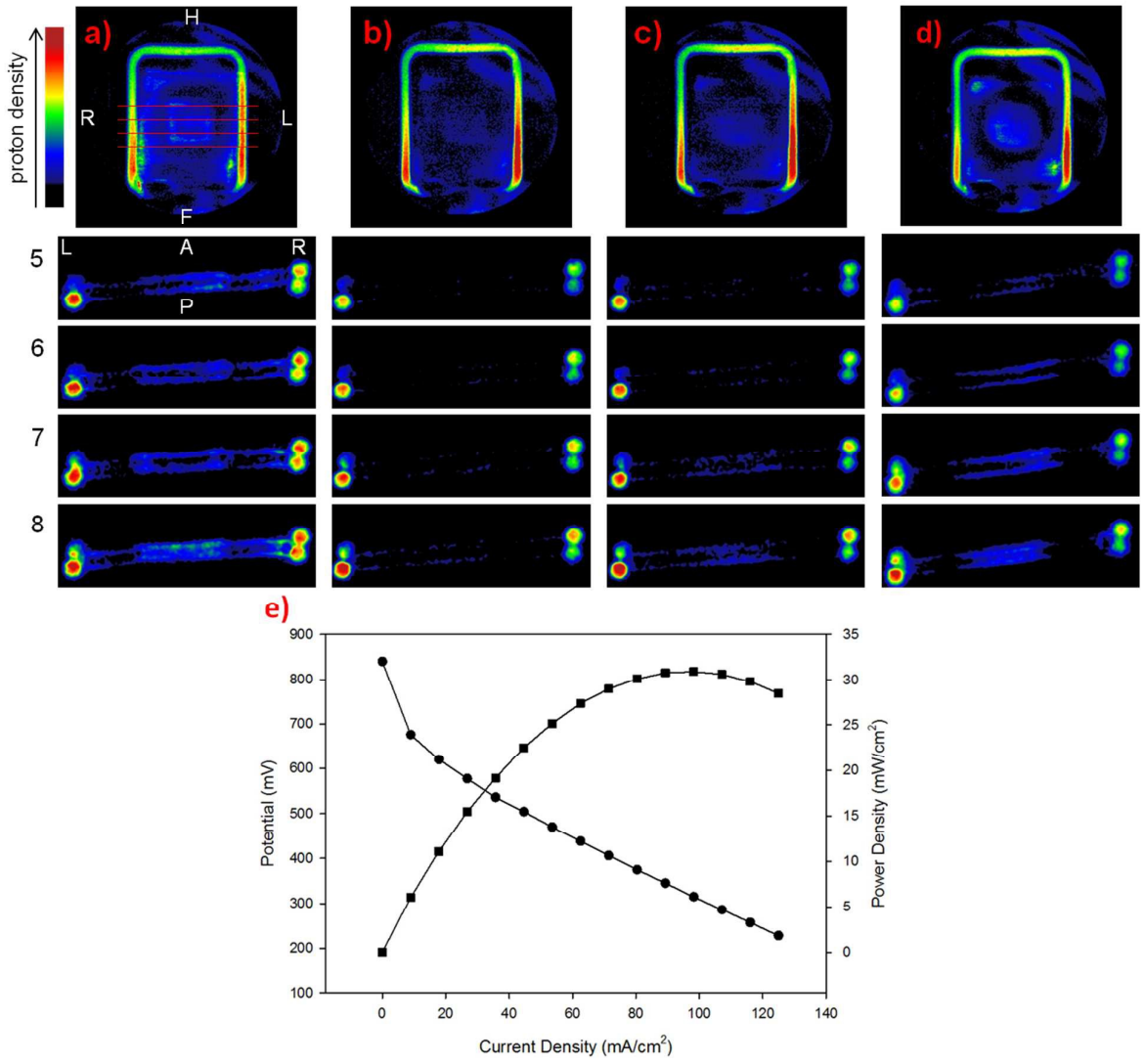

Fig. 2 a)-d) ^{1}H ZTE images and axial slices extracted from the corresponding 3D dataset (see ESI, Fig. S5) obtained from the PBI_5N MEA operating with H_2 (0.3L/min) and air (5L/min) at 80°C (humidity lower than 50%. FOV: 4x4x4cm, resolution: 0.208mm/pixel). During operation the current was maintained constant at 30mA. a) fuel cell at 25°C before operation (0mA, 0V); b) t=0 (80°C, 30mA, 0.44V); c) t=420min (80°C, 30mA, 0.42V); d) fuel cell at 25°C 14 hours after the switch off at 420 min; e) polarization curve of the cell at 80°C. In the slices the anode can be seen in the upper part (anterior side (A)).

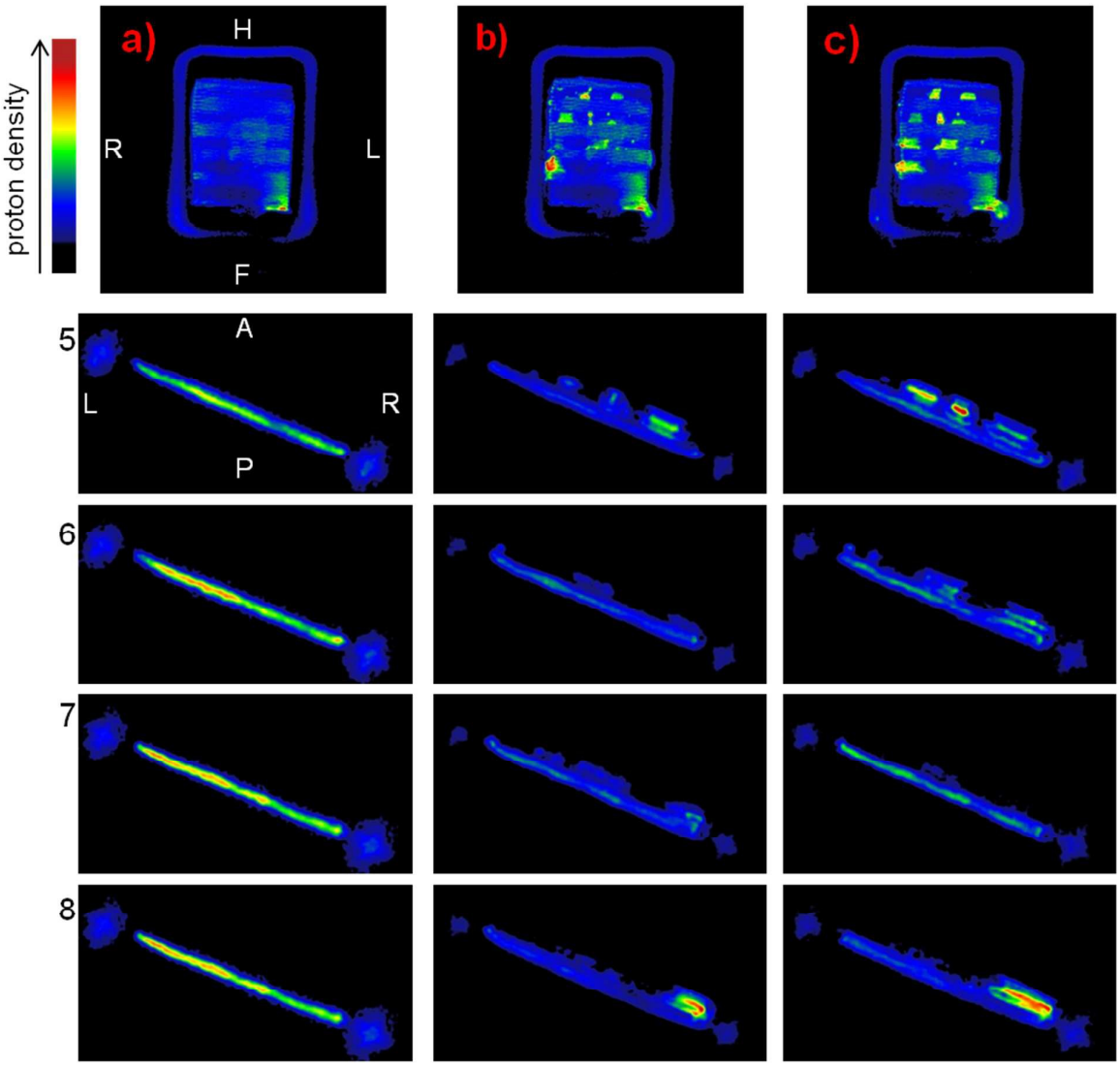

Fig. 3 a)-c) ^{1}H ZTE images and axial slices extracted from the corresponding 3D dataset obtained from the PBI_5N fuel cell operating at 35°C. During operation the current was maintained constant at 5mA. a) fuel cell at 35°C before operation (0mA, 0V); b) t=60min (5mA, 0.39V); c) t=120min (5mA, 0.33V). In the slices the anode can be seen in the upper part (A).

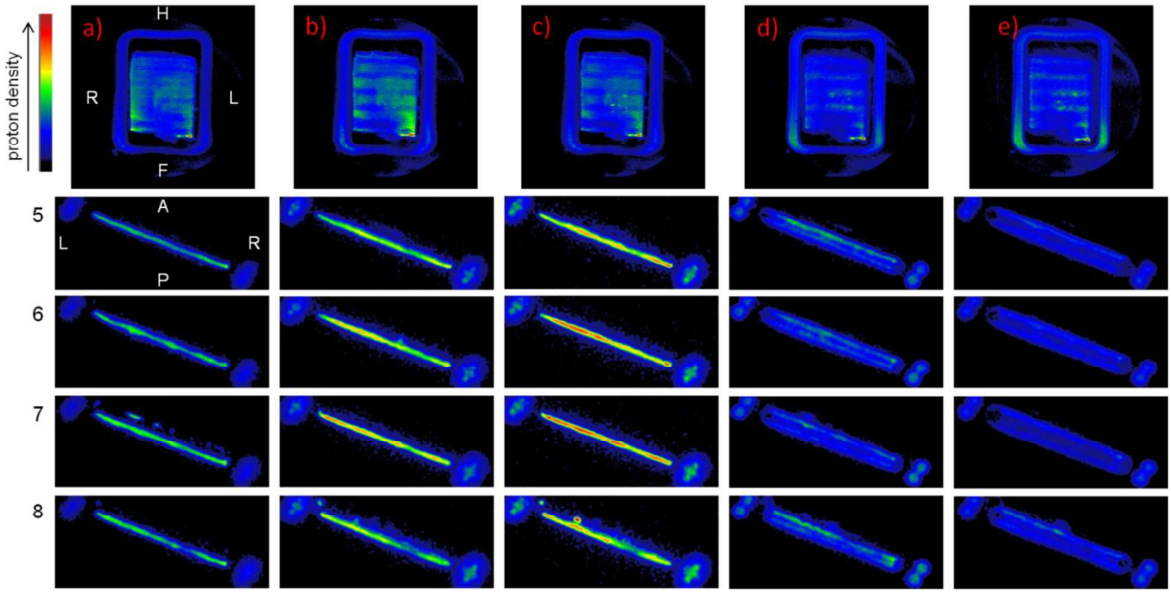

Fig. 4 a)-e) ^{1}H ZTE images and axial slices extracted from the corresponding 3D dataset obtained from the PBI_5N fuel cell operating at 47°C. During operation the current was maintained constant at 5mA. a) fuel cell at 25°C before operation (0mA, 0V); b) t=10min (47°C, 5mA, 0.43V); c) t=75min (47°C, 5mA, 0.33V); d) t=135min (47°C, 5mA, 0.29V); e) t=255min (47°C, 5mA, 0.21V). In the slices the anode can be seen in the upper part (A).